BIOCHEMISTRY
including biophysical chemistry & molecular biology
Rapid Report

Biochemistry **2009,** *48,* 3801–3803 3801
DOI:10.1021/bi900308c

Monitoring the Interaction of a Single G-Protein Key Binding Site with Rhodopsin Disk Membranes upon Light Activation†

Tai-Yang Kim,‡ Hiroshi Uji-i,§ Martina Möller,‡ Benoit Muls,§ Johan Hofkens,§ and Ulrike Alexiev*,‡

‡*Physics Department, Freie Universität Berlin, Arnimallee 14, D-14195 Berlin, Germany, and* §*Division of Molecular and Nano Materials, Katholieke Universiteit Leuven, Celestinienlaan 200F, 3001 Leuven, Belgium*

Received February 22, 2009. Revised Manuscript Received March 19, 2009

ABSTRACT: Heterotrimeric G-proteins interact with their G-protein-coupled receptors (GPCRs) via key binding elements comprising the receptor-specific C-terminal segment of the α-subunit and the lipid anchors at the α-subunit N-terminus and the γ-subunit C-terminus. Direct information about diffusion and interaction of GPCRs and their G-proteins is mandatory for an understanding of the signal transduction mechanism. By using single-particle tracking, we show that the encounters of the α-subunit C-terminus with the GPCR rhodopsin change after receptor activation. Slow as well as less restricted diffusion compared to the inactive state within domains 60−280 nm in length was found for the receptor-bound C-terminus, indicating short-range order in rhodopsin packing.

G-Protein-coupled receptors (GPCRs) constitute a large superfamily of membrane receptors responsible for the transduction of various external stimuli (*1*). In rhodopsin, a prototype of GPCR subfamily A, the reception of light and subsequent signal mediation across the membrane leads to conformational changes in the receptor, facilitating molecular recognition between the active Metarhodopsin-II (Meta-II) intermediate and the G-protein transducin on the cytosolic face of the receptor (*2*). The specialization of rhodopsin in phototransduction is reflected in its structure and cellular arrangement: High concentrations of the receptor in the stacked disks located in the rod outer segments (ROS) are combined with a lack of most of the other proteins involved in cellular function and ultrafast switching from the covalently bound inactive (11-*cis*-retinal) to the active ligand (*all-trans*-retinal). The packing properties of rhodopsin in the disk membrane and the diffusional characteristics of transducin will affect the timing of events in the complex signal transduction cascade. Simulations of stochastic encounters between light-activated rhodopsin and transducin reveal a clear dependence on rhodopsin packing and lateral diffusion of transducin; a respective high lateral diffusion coefficient of transducin seems to be sufficient to obtain the fast responses required, even at high concentrations of immobile rhodopsins (*3*). However, the packing of rhodopsin in the membrane and the related diffusion coefficients are controversially discussed. While early experiments indicated that rhodopsin diffuses freely in the lipid bilayer of the disk membrane (*4*), recent atomic force microscopy data revealed rows of rhodopsin dimers in a paracrystalline lattice (*5*), an arrangement which seems to conflict with a freely diffusing rhodopsin. Thus, direct information about the diffusion and interaction properties of rhodopsin and transducin is mandatory for deducing the underlying microscopic principle of action. To the best of our knowledge, direct measurements of lateral diffusion behavior of transducin on the single-molecule level were not reported, so we set out to implement a setup based on single-molecule tracking to follow the encounters and lateral diffusion of transducin and its binding elements with the disk membrane.

Here we performed a proof-of-principle experiment to show the feasibility of the single-molecule spectroscopy approach to studying the time dependence of the light-triggered interaction between rhodopsin and transducin. For a clear-cut discrimination between the different interaction modes in the dark and light-activated state of rhodopsin, we took advantage of the fact that transducin (G_T)-derived peptides of the $G_T\alpha$-subunit C-terminus recognize the active form of the receptor and can replace holotransducin in stabilizing Meta-II (*6*). In particular, the peptide derived from the extreme C-terminus of the $G_T\alpha$-subunit has supposedly no affinity for dark rhodopsin (*7*) but high affinity for light-activated rhodopsin (*6*,*7*). Thus, this peptide is expected to show membrane interaction only after light activation, in contrast to holotransducin with its lipid anchors. A recent crystal structure highlights the interaction of the transducin peptide with an active state of the receptor (*8*) (Figure 1C).

For our experiments, we used a fluorescently labeled variant of the C-terminal segment of the $G_T\alpha$-subunit, $pG_T\alpha$-F (F is the fluorescence label Atto647N). In the initial experiment, we followed the interaction of $pG_T\alpha$-F with inactive (dark) rhodopsin membranes using single-molecule wide-field microscopy (*9*). As rhodopsin membrane sheets are known to form well-defined layer

†This work was partially supported by the German Science Foundation, the FWO, Katholieke Universiteit Leuven, and the Flemish government.

*To whom correspondence should be addressed. Phone: ++49-30-838-55157. Fax: ++49-30-838-56510. E-mail: alexiev@physik.fu-berlin.de.

Published on Web 3/20/2009

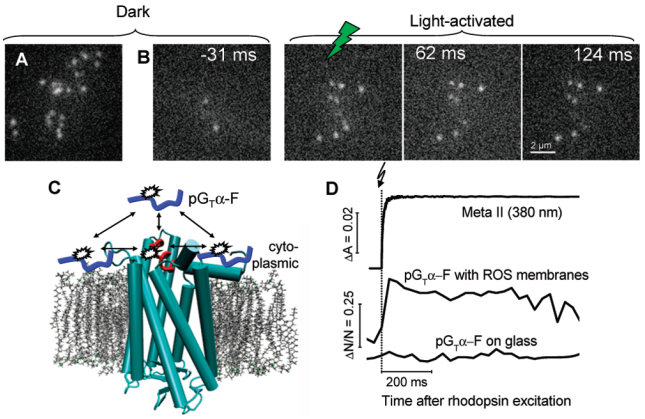

FIGURE 1: Fluorescence images of single $pG_T\alpha$-F. (A) Interaction with dark rhodopsin (ROS) membranes. (B) Image series from the time-resolved interaction of $pG_T\alpha$-F with light-activated disk membranes. Same area as in panel A but with a reduced amount of fluorescent $pG_T\alpha$-F. (C) Structure of opsin (cyan) in complex with the C-terminal peptide of the transducin α-subunit (red) (*8*), together with receptor-unbound fluorescently labeled peptides (blue). (D) Kinetics of Meta-II formation (*20*) and increase in the number (*N*) of interacting $pG_T\alpha$-F molecules after rhodopsin light activation. Conditions: 130 mM NaCl, 10 mM MES, pH 6, 19 °C.

structures (*10*), we deposited disk membrane layers at the surface of a glass coverslip in a buffer-filled sample compartment. The fluorescently labeled $pG_T\alpha$ molecules are visible as bright spots when added to the nonlabeled rhodopsin disk membranes. With increased $pG_T\alpha$-F concentrations, areas of high $pG_T\alpha$-F localization were observed (Figure 1A), consistent with the outline of individual membrane patches. In control experiments without membranes, we observed a homogeneous interaction pattern (data not shown). To allow for a visualization of the expected increase in the number of $pG_T\alpha$-F molecules interacting with the activated rhodopsin, we reduced the number of fluorescent $pG_T\alpha$-F molecules sufficiently (Figure 1B, first image). Figure 1B presents an image series from the first time-resolved observation of the interaction and diffusion characteristics of $pG_T\alpha$-F with disk membranes and their changes upon light activation. An integration time of 31 ms per frame (32 Hz) was used. The image series starts with the frame before the green flash activates rhodopsin and clearly shows that rhodopsin activation triggers an increase in the number of interacting $pG_T\alpha$-F molecules. This increase was absent without rhodopsin membranes (Figure 1D). Within the first frame after the flash, the highest number of $pG_T\alpha$-F molecules was observed at the membrane surface. Thus, initial binding occurs within the formation time of Meta-II (Figure 1D). This is fast compared to the binding kinetics in the time range of seconds observed for mass-tagged C-terminal segments in classical light scattering experiments (*7*), but comparable with the binding time constant of G_T (40 ms) in earlier reports (*11*). The observation of light-induced binding of single $pG_T\alpha$-F molecules to rhodopsin disk membranes was a crucial test for the successful application of single-molecule fluorescence spectroscopy.

To further quantify the wide-field single-molecule fluorescence experiments, we analyzed the mobility of $pG_T\alpha$-F molecules. As the G_T-derived peptide interacts tightly with the receptor after rhodopsin light activation (*6*), it is expected to report on the mobility of the active Meta-II molecule. Mean square displacements ($\langle r^2 \rangle$) obtained from $pG_T\alpha$-F trajectories are presented for several molecules before and after rhodopsin light activation (Figure 2B,E). The distribution of the distances *r* (step length) a molecule moves in a given time allows for the detection of subpopulations in nonhomogeneous populations (*12*, *13*). Nonhomogeneous populations are suspected from the $\langle r^2 \rangle$ plot and are indicated in Figure 2B,E with different colors. The step length distributions for inactive and light-activated rhodopsin membranes can be satisfactorily described by a biexponential fit, yielding two subpopulations (Figure 2C,F). In the dark state of rhodopsin, we observed that ~70% of the $pG_T\alpha$-F molecules interact only for one frame with the disk membranes (Figure 2A), consistent with the vanishing affinity of the peptidic binding element for inactive rhodopsin. Less than 20% of the molecules contribute to the trajectories and the step length distribution shown in Figure 2B,C. The time dependence of the coefficients from the distribution functions reveals that the r^2 values of the major fraction are constant and close to the displacement accuracy of our experiment, thus indicating immobile $pG_T\alpha$-F. As a fit to the decaying residence time histogram (Figure S3A) results in a time constant of 49 ms, those molecules which interact for two frames were analyzed separately. They display a higher mobility: $r_1^2 = (6.0 \pm 1.2) \times 10^{-3}\ \mu m^2$, and $r_2^2 = (47 \pm 1.2) \times 10^{-3}\ \mu m^2$. According to the relationship $r^2 = 4Dt$ for normal diffusion, this yields the following diffusion constants: $D_1 = 0.05\ \mu m^2/s$, and $D_2 = 0.38\ \mu m^2/s$. The situation is different after light activation of rhodopsin. The percentage of molecules, which interact for only one frame, is reduced to ~40% (Figure 2D), consistent with the fact that the majority of $pG_T\alpha$-F tightly binds to active rhodopsin. However, rhodopsin light activation surprisingly results in an increased heterogeneity in $pG_T\alpha$-F mobility (Figure 2E). More mobile components are evident from the step length distribution histogram (Figure 2F, orange fit) and the corresponding cumulative distribution function (Figure 3A). The fractional amplitude of the fast component is increased from ~0.2 in the dark to ~0.5 after light activation (Figure 3A,B). While for

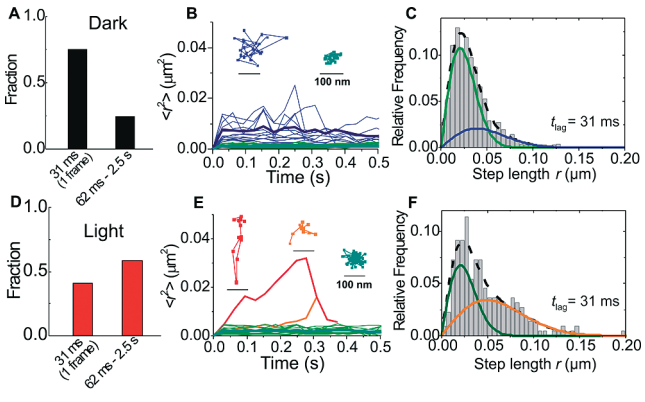

FIGURE 2: Residence times and time dependence of $\langle r^2 \rangle$. Dark rhodopsin membranes. (A) Residence times of interacting $pG_T\alpha$-F with dark disk membranes. (B) Mean square displacements: thick lines, mean of respectively colored time traces; inset, selected tracks. (C) Step length distribution. Fit (dashed line): $r_1^2 = 0.0009 \pm 0.0001\ \mu m^2$ (green); $r_2^2 = 0.003 \pm 0.001\ \mu m^2$ (blue). Light-activated rhodopsin membranes. (D) Residence times of interacting $pG_T\alpha$-F with light-activated disk membranes. (E) Mean square displacements: bold, mean of respectively colored time traces; inset, selected tracks. (F) Step length distribution. Fit: $r_1^2 = 0.001 \pm 0.0001\ \mu m^2$ (green); $r_2^2 = 0.005 \pm 0.001\ \mu m^2$ (orange).

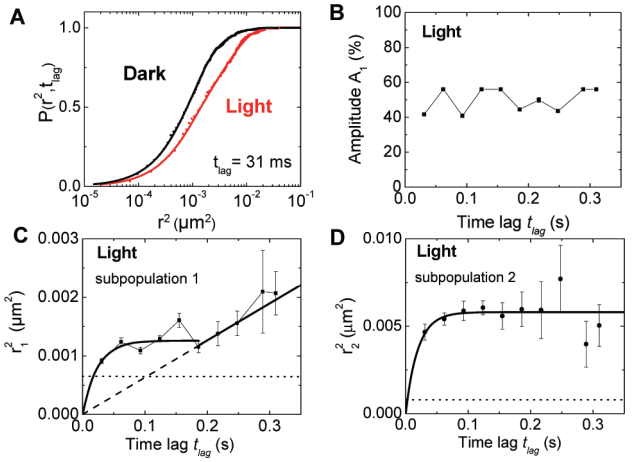

FIGURE 3: Time dependence of distribution function coefficients. (A) Probability distribution function for square displacements of $pG_T\alpha$-F interacting with dark (black; fit, $r_1^2 = 0.0009\ \mu m^2$, $r_2^2 = 0.0037\ \mu m^2$, $A_1 = 0.81$) and light-activated (red; fit, $r_1^2 = 0.001\ \mu m^2$, $r_2^2 = 0.0047\ \mu m^2$, $A_1 = 0.42$) rhodopsin membranes. For immobile $pG_T\alpha$-F, $r^2 = 0.0002\ \mu m^2$. (B) Time lag dependence of amplitude A_1 (slow fraction) after rhodopsin light activation. (C) Time lag dependence of r^2 (slow component) after rhodopsin light activation from a selected experiment (fit, $L_1 = 61 \pm 2$ nm, $D_0 = 0.01\ \mu m^2/s$). (D) Time lag dependence of r^2 (fast component) after rhodopsin light activation from a selected experiment (fit, $L_2 = 130 \pm 2$ nm, $D_0 = 0.1\ \mu m^2/s$). The dotted horizontal line in panels C and D represents the mean displacement accuracy.

the dark rhodopsin membranes strongly confined diffusion and immobilization of interacting $pG_T\alpha$-F were observed, the time dependence of the r^2 values after light activation indicates less restricted diffusion (Figure 3C,D). Restricted diffusion behavior (*14*) may be explained by a confined diffusion model (*15*). The confinement lengths (L) are between 60 nm (subpopulation 1) and 280 nm (subpopulation 2), depending on the sample, with the following initial diffusion constants: $D_0 = 0.01\ \mu m^2/s$, and $D_0 = 0.1\ \mu m^2/s$, respectively. More interestingly, subpopulation 1 displays an increase in r^2 with time, starting about 200 ms after light activation of rhodopsin. This suggests a change to normal diffusion with a D of $0.002\ \mu m^2/s$ (Figure 3C). This phenomenon was observed in all experiments (three different samples). We propose that the observed transition to normal diffusion after rhodopsin light activation is caused by slow diffusion of the receptor detected through rhodopsin-bound $pG_T\alpha$-F molecules. The change in diffusion behavior is probably induced by alterations in rhodopsin packing, supported by the observed increase in confinement length after light activation, and by structural changes in activated rhodopsin. Studies on rhodopsin oligomerization suggest that rhodopsin tends to oligomerize, and simulations predict short-range order in rhodopsin membrane assembly (*16*, *17*). A recent fluorescence recovery after photobleaching study (*18*) on G_T and rhodopsin in tadpole rods found high mobility for activated, G-protein-devoid rhodopsin, but sequestration into cholesterol-dependent microdomains for the G_T-bound receptor. The diffusion constant of the latter ($0.05\ \mu m^2/s$) is within the range of the D_0 values found here for the activated receptor-bound $pG_T\alpha$-F. Only those $pG_T\alpha$-F which briefly interact with the inactive membrane display higher mobility ($D \sim 0.4\ \mu m^2/s$). We suggest that these high-mobility molecules probably interact with the lipid phase, as mobile G-protein lipid anchors displayed diffusion coefficients in the same range (*19*).

Taken together, our single-molecule tracking data support the conclusion that membrane microdomains play a role in the organization of GPCRs. In the case of rhodopsin, single light-activated receptors diffuse in membrane domains of different sizes at a time scale of milliseconds to seconds. This suggests disk membrane inhomogeneity and is compatible with a semiordered packing of rhodopsin over a time range which corresponds to the millisecond activation time scale of rhodopsin. The successful visualization of the light-induced interaction of a single transducin binding element with rhodopsin opens the possibility to further investigate diffusion characteristics and interactions of holotransducin and its subunits on the single-molecule level to provide deeper insights into the regulation of receptor−G-protein activation. Within a greater scheme, the interaction and the mutual interference with molecules controlling the multistep shutoff of activated rhodopsin can be directly visualized, and their dynamics in the signaling cascade can be studied in the future.

ACKNOWLEDGMENT

We thank Dr. Sebastian Haase for performing the test with simulated data.

SUPPORTING INFORMATION AVAILABLE

Details of experimental procedures and data analysis. This material is available free of charge via the Internet at http://pubs.acs.org.

REFERENCES

1. Bockaert, J., and Pin, J. P. (1999) *EMBO J. 18*, 1723–1729.
2. Sakmar, T. P., Menon, S. T., Marin, E. P., and Awad, E. S. (2002) *Annu. Rev. Biophys. Biomol. Struct. 31*, 443–484.
3. Dell'Orco, D., and Schmidt, H. (2008) *J. Phys. Chem. B 112*, 4419–4426.
4. Poo, M., and Cone, R. A. (1974) *Nature 247*, 438–441.
5. Fotiadis, D., Liang, Y., Filipek, S., Saperstein, D. A., Engel, A., and Palczewski, K. (2003) *Nature 421*, 127–128.
6. Kisselev, O. G., Meyer, C. K., Heck, M., Ernst, O. P., and Hofmann, K. P. (1999) *Proc. Natl. Acad. Sci. U.S.A. 96*, 4898–4903.
7. Herrmann, R., Heck, M., Henklein, P., Henklein, P., Kleuss, C., Hofmann, K. P., and Ernst, O. P. (2004) *J. Biol. Chem. 279*, 24283–24290.
8. Scheerer, P., Park, J. H., Hildebrand, P. W., Kim, Y. J., Krauss, N., Choe, H. W., Hofmann, K. P., and Ernst, O. P. (2008) *Nature 455*, 497–502.
9. Rocha, S., Hutchison, J. A., Peneva, K., Herrmann, A., Müllen, K., Skjøt, M., Jørgensen, C. I., Svendsen, A., De Schryver, F. C., Hofkens, J., and Uji-I, H. (2009) *ChemPhysChem 10*, 151–161.
10. Fitter, J., Ernst, O. P., Hauss, T., Lechner, R. E., Hofmann, K. P., and Dencher, N. A. (1998) *Eur. Biophys. J. 27*, 638–645.
11. Bennett, N., Michel-Villaz, M., and Kühn, H. (1982) *Eur. J. Biochem. 127*, 97–103.
12. Kues, T., Dickmanns, A., Lührmann, R., Peters, R., and Kubitscheck, U. (2001) *Proc. Natl. Acad. Sci. U.S.A. 98*, 12021–12026.
13. Schütz, G. J., Schindler, H., and Schmidt, T. (1997) *Biophys. J. 73*, 1073–1080.
14. Saxton, M. J., and Jacobson, K. (1997) *Annu. Rev. Biophys. Biomol. Struct. 26*, 373–399.
15. Kusumi, A., Sako, Y., and Yamamoto, M. (1993) *Biophys. J. 65*, 2021–2040.
16. Periole, X., Huber, T., Marrink, S.-J., and Sakmar, T. P. (2007) *J. Am. Chem. Soc. 129*, 10126–10132.
17. Botelho, A. V., Huber, T., Sakmar, T. P., and Brown, M. F. (2006) *Biophys. J. 91*, 4464–4477.
18. Wang, Q., Zhang, X., Zhang, L., He, F., Zhang, G., Jamrich, M., and Wensel, T. G. (2008) *J. Biol. Chem. 283*, 30015–30024.
19. Perez, J.-P., Segura, J.-M., Abankwa, D., Piguet, J., Martinez, K. L., and Vogel, H. (2006) *J. Mol. Biol. 363*, 918–930.
20. Alexiev, U., Rimke, I., and Pöhlmann, T. (2003) *J. Mol. Biol. 328*, 705–719.